



HAL
open science

G protein-coupled receptors can control the Hippo/YAP pathway through Gq signaling

Diana Zindel, Patrick Mensat, Claire Vol, Zeinab Homayed, Fabienne Charrier-savournin, Eric Trinquet, Jean-louis Banères, Jean-Philippe Pin, Julie Pannequin, Thomas Roux, et al.

► To cite this version:

Diana Zindel, Patrick Mensat, Claire Vol, Zeinab Homayed, Fabienne Charrier-savournin, et al.. G protein-coupled receptors can control the Hippo/YAP pathway through Gq signaling. *FASEB Journal*, 2021, 35 (7), pp.e21668. 10.1096/fj.202002159R . hal-03263933

HAL Id: hal-03263933

<https://hal.science/hal-03263933>

Submitted on 18 Nov 2021

HAL is a multi-disciplinary open access archive for the deposit and dissemination of scientific research documents, whether they are published or not. The documents may come from teaching and research institutions in France or abroad, or from public or private research centers.

L'archive ouverte pluridisciplinaire **HAL**, est destinée au dépôt et à la diffusion de documents scientifiques de niveau recherche, publiés ou non, émanant des établissements d'enseignement et de recherche français ou étrangers, des laboratoires publics ou privés.

G protein-coupled receptors can control the Hippo/YAP pathway through Gq signaling

Diana Zindel¹, Patrick Mensat², Claire Vol¹, Zeinab Homayed¹, Fabienne Charrier-Savournin², Eric Trinquet², Jean-Louis Banères³, Jean-Philippe Pin¹, Julie Pannequin¹, Thomas Roux², Elodie Dupuis², Laurent Prézeau^{1*}

1 Institut de Génomique Fonctionnelle (IGF), Univ. Montpellier, CNRS, INSERM, Montpellier, France.

2 Perkin-Elmer/CisBio, Codolet, France.

3 Institut des Biomolécules Max Mousseron, Univ. Montpellier, CNRS, Montpellier, France.

* Corresponding author: Laurent Prézeau, IGF, 141 rue de la Cardonille, 34094 Montpellier Cedex 5, France – email: laurent.prezeau@igf.cnrs.fr – tel : +33(0)4 34359296

Running title: GPCR-induced dual regulation of YAP through Gq

Nonstandard abbreviations:

AMOT	Angiomotin
AMPK	AMP-Activated Protein Kinase
cAMP	cyclic Adenosin MonoPhosphate
CTGF	Connective Tissue Growth Factor
CYR61	Cystein-Rich Angiogenic Protein 61
ECM	Extra-Cellular Matrix
FAK	Focal Adhesion Kinase
FRET	Förster Resonance Energy Transfer
GHS	Growth Hormone Secretagogue protein
GPCR	G Protein-Coupled Receptor
GPER	GPCR Estrogen Receptor
GTPase	Guanosine TriPhosphate hydrolase
HEK293	Human Embryonic Kidney 293 cells
HTRF®	Homogenous Time-Resolved FRET
IP1	Inositol-Phosphate 1
LATS	Large Tumor Suppressor Kinase
LiCl	Lithium Chloride
MST	Mammalian Sterile20-like protein
NF2	Neurofibromin 2
PLC	Phospholipase C
PTX	Pertussis Toxin
S1P	Sphingosin-1-Phosphate
SPA	Substance P Analogue
TAZ	Tafazzin
TEAD	Transcriptional Enhanced Associate Domain factor
TR-FRET	Time-Resolved FRET
YAP	YES-Associated Protein

Acknowledgements

The pharmacology, BRET, and FRET experiments were performed using the ARPEGE Pharmacology-Screening-Interactome platform facility (UMS Biocampus), Montpellier, France. We thank Sylvain Jeannot of the team of Sébastien Granier (IGF) for his technical help.

Conflicts of interest

Authors have no conflicts of interest.

Author contributions

ZD – Experimental data, Data analysis, Manuscript writing

PM – Experimental data, Data analysis

CV – Experimental data, Data analysis

ZH – Experimental data, Data analysis

FCS – Providing cell line and Cisbio products, Cisbio Data analysis

ET – Cisbio Data analysis, Manuscript correction

JLB – Providing agonist and inverse agonist compounds, Manuscript correction

JPP – Data analysis, manuscript writing

JP – Technical and experimental training, Manuscript correction

TR – Cisbio products, Cisbio Data analysis

ED – Providing Cisbio data and products, Cisbio Data analysis, Manuscript correction

LP – Project initiation and supervision, Data analysis, Manuscript writing

Abstract

The Hippo pathway is an evolutionary conserved kinase cascade involved in the control of tissue homeostasis, cellular differentiation, proliferation, and organ size, and is regulated by cell-cell contact, apical cell polarity, and mechanical signals. Miss-regulation of this pathway can lead to cancer. The Hippo pathway acts through the inhibition of the transcriptional coactivators YAP and TAZ through phosphorylation. Among the various signaling mechanisms controlling the hippo pathway, activation of G12/13 by G protein coupled receptors (GPCR) recently emerged. Here we show that a GPCR, the ghrelin receptor, that activates several type of G proteins, including G12/13, Gi/o, and Gq, can activate YAP through Gq/11 exclusively, independently of G12/13. We revealed that a strong basal YAP activation results from the high constitutive activity of this receptor, that can be further increased upon agonist-activation. Thus, acting on ghrelin receptor allowed to modulate up-and-down YAP activity, as activating the receptor increased YAP activity and blocking constitutive activity reduced YAP activity. Our results demonstrate that GPCRs can be used as molecular switches to finely up- or down-regulate YAP activity through a pure Gq pathway.

Keywords:

Hippo pathway

Cellular Signaling

Constitutive activity

Inverse agonist

Ghrelin receptor

Introduction

The Hippo pathway originally identified in *Drosophila* is an evolutionary conserved kinase cascade playing essential roles in tissue homeostasis, cellular differentiation, proliferation, and organ size control [1,2]. Core components of this signaling cascade in vertebrates comprise the Ser/Thr-kinase MST1/2 that phosphorylates large tumor suppressor kinase LATS1/2 when associated with Sav1 [3]. In turn LATS1/2 deactivates the two downstream effector proteins YAP and TAZ by phosphorylation, notably Ser127 of YAP [4], leading to their retention in the cytosol by an interaction with 14-3-3 proteins and to their degradation. Conversely, dephosphorylated YAP/TAZ act as transcriptional coactivators by translocating into the nucleus and binding mainly to the TEAD family of transcription factors to modify gene expression. Among their targets are genes that inhibit apoptosis and promote proliferation such as connective tissue growth factor (CTGF) or cysteine-rich angiogenic inducer 61 (CYR 61) [5,6]. According to its physiological functions, mis-regulation of the Hippo pathway triggers pathological processes leading to tumorigenesis [7–10]. Thus, strong YAP/TAZ activity, often indicative of poor prognosis, has been reported in colon, liver, breast and ovarian cancers, and melanomas [11–14]. YAP/TAZ even regulate the fate and self-renewal of cancer stem cells in colon and breast cancers, and may contribute to mechanisms of resistance to therapeutic treatments [15–17]. YAP/TAZ axis plays also a role in regulating cell metabolism [18], as expression and activity of YAP/TAZ are regulated by glucose, fatty acids, nutrients, and hormones, while YAP/TAZ modulate glycolysis and lipogenesis. Moreover, YAP can be inhibited by AMPK-mediated cellular energy stress [19], due to direct phosphorylation of YAP Ser94 by AMPK or to AMPK-dependent activation of LATS, suppressing the oncogenic transformation in cells deficient of LATS. All these Hippo axis complex actions are under the control of numerous upstream molecular regulators [20].

Hippo YAP/TAZ axis activity underlying its physio-pathological actions is then under the control of numerous inputs, like cell-cell contact inhibition at tight and adherent junctions [21], apical cell polarity [22], or mechanical signals induced by extracellular matrix (ECM) rigidity and cell shape [23]. These biophysical events are relayed by membrane molecular complexes like integrins-based focal adhesion complexes that mostly control cytoskeleton organization and intracellular Rho pathway down to YAP/TAZ activation. At adherent junctions, the protein Neurofibromatosis 2 (NF2/Merlin) interact with membrane α -catenin and Angiomotin (AMOT), the later recruiting LATS1/2 and YAP, facilitating YAP phosphorylation by LATS 1/2 [24]. Besides mechanical cues, strong evidence for Hippo pathway regulation by membrane G protein-coupled receptor (GPCR) has recently emerged as a major focus in the field [25].

GPCRs can increase or inhibit YAP/TAZ activity depending on the heterotrimeric G-protein mobilized by the GPCR [25–27]. Gs G protein activation induces YAP phosphorylation and thereby inactivates the YAP/TAZ pathway [25], as recently illustrated in skin cancer cells [28]. Indeed, activation of the Protein kinase dependent on cAMP (PKA) blocks YAP activity through the direct stimulation of LATS1/2 kinase or indirectly through the phosphorylation of the tumor suppressor protein NF2/Merlin making NF2 able to interact with and activate LATS1/2. In contrast to the Gs tumor suppressor action, it is now established that G12/13 G proteins activation promotes YAP activation, nuclear translocation, and gene expression activity, via the Rho GTPase cascade [25,27,29–32], as first illustrated with the Sphingosin-1 phosphate receptor S1P2 [25,27]. In this complex cascade, RhoA GTPase controls F-actin polymerization that can then bind AMOT, competing with LATS1/2 interaction on AMOT. The released inactive LATS1/2 is then unable to phosphorylate YAP. While many GPCRs activate YAP mainly or exclusively through G12/13, the role of other G proteins remains unclear.

In the present study, we show that a GPCR known to activate both G12/13 and Gq types of G proteins can regulate YAP/TAZ activity via Gq exclusively. Indeed, basal and agonist-induced activity of this receptor can inhibit YAP phosphorylation, promoting its activity, while an inverse agonist favors its phosphorylation. This effect is prevented by Gq inhibitors, while G12/13 knock-down have no effect. These data then reveal a novel way GPCRs can regulate this important signaling cascade.

Materials and Methods

Reagents

The HTRF[®] kits to detect either phosphorylation of YAP on the S127 residues or total YAP relative protein amount were developed by Cisbio ([35] and <https://fr.cisbio.eu/>, Cisbio, Codolet, France) in collaboration with Laurent Prézeau and Jean-Philippe Pin. Reagents were purchased from Tocris unless otherwise specified. MK0677 was purchased from Axon Medchem. JMV-5289 and JMV-3011 were synthesized by Dr. Jean-Alain Fehrentz (IBMM, université Montpellier, France) as described elsewhere [33].

Cell culture and stable expression in HEK 293 cells

GHS-R1a stable HEK293 cell line (#C1SU1GHSR1A) is a commercial cell line generated by Perkin-Elmer/Cisbio (<https://fr.cisbio.eu/> and [34]). Cells were maintained in Dulbecco's modified Eagle's medium supplemented with 10% (V/V) fetal calf serum, penicillin (50 mg/ml), and streptomycin (50 mg/ml). Cells were used for experiments at intermediate cell density, to avoid inhibition of YAP/TAZ activity due to cell-cell contacts. The GHS-R1a receptor was tagged with the SNAP domain, allowing labelling as described in the SUPP-legend section.

siRNA

Gα12, Gα13, and control siRNAs were purchased from the Dharmacon SMART pool (Dharmacon, ThermoFischer Scientific, Illkirch, France). HEK293 cells were transiently transfected with siRNA using DharmaFECT 1 (Dharmacon) transfection reagent according to the manufacturer's protocol.

qPCR primer sequences

Gene	Primer sequence (5'-3')
GNA12	F: GGAGGGATTCTGGCATCAGG R: CCGATCCGGTCCAAGTTGTC
GNA13	F: TCCCTGGGGAGACAACTCAA R: TTTCCACCATTCCCTTGGGCTG
CYR 61	F: GGTCAAAGTTACCGGGCAGT R: GGAGGCATCGAATCCCAGC
CTGF	F: AAAAGTGCATCCGTACTCCCA R: CCGTCGGTACATACTCCACAG

GAPDH

F: TCATTGACCTCAACTACATGGTTT

R: GAAGATGGTGATGGGATTTTC

YAP phosphorylation

HTRF®-based assays were developed to detect phosphorylation of YAP on its Serine 127 residues (Phospho-YAP (S127) HTRF® kit, #64YATPEG), and the relative amount of YAP protein (Total-YAP HTRF® kit, #64YAPPEG) ([35] and <https://fr.cisbio.eu/>). In the Total-YAP HTRF® kit, two antibodies recognizing the YAP protein on different epitopes are labelled with either a Time-Resolved Forster Resonance Energy Transfer (TR-FRET) donor lumiphore (Europium cryptate), or with a TR-FRET acceptor lumiphore (D2 lumiphore). When both labelled antibodies are bound to the YAP protein, the activation of the donor lumiphore with a 337 nm laser leads to a transfer of energy from its energetic states to the acceptor compatible energetic states that results in an emission of light at 665 nm. In any other case, there is no energy transfer and only the emission of the activated donor is detected (620m). Similarly, in the case of the Phospho-YAP (S127) HTRF® kit, two HTRF® compatible lumiphore labelled antibodies were used, one antibody recognizing the YAP protein and the other one only the S127-phosphorylated YAP protein. Measurement of phosphorylated and total YAP was performed in HEK293 cells, starved overnight. The cells were stimulated with the indicated ligands, then both antibodies were added, and the read was performed after overnight incubation later using either the luminometers Pherastar (BMGLabtech) or Spark (TECAN). The HTRF® ratio was calculated as the ratio of the sensitized acceptor signal integrated in time window 50–500 µs over donor signal integrated over the same time window and multiplied by 10 000.

Inositol phosphate production

Inositol phosphate production level was measured in HEK293 cells thanks to the HTRF® IPOne -Gq kit (Perkin-Elmer/Cisbio, Codolet, France) as described previously [36]. Briefly, the HTRF® IPOne -Gq kit is a competitive immunoassay that uses a Terbium cryptate-labelled anti-IP1 monoclonal antibody and d2-labeled IP1 (IP1-d2) generating a TR-FRET signal. Then, any IP1 produced by the cells will compete with the labelled IP1-d2 and induce a decrease in TR-FRET signal. LiCl is added to the cell-stimulation buffer, causing the accumulation of IP1 upon receptor activation. Prior to lysis and the addition of the IP1-Tb antibody and IP1-d2, receptor-transfected HEK293 cells were treated with the indicated test compounds. The receptor-transfected cells were then stimulated with the indicated ligands. The cell lysates were transferred to a 384-well plate, and both antibodies were added; the read was performed 2 h

later using either the luminometers Pherastar (BMG) or Spark (TECAN) for HTRF® ratio determination according to the manufacturer recommendations. The HTRF® ratio was calculated as the ratio of the sensitized acceptor signal integrated in time window 50–500 µs over donor signal integrated over the same time window and multiplied by 10 000.

Immunostaining

HEK293 cells were grown on poly-L-Ornithine glass coverslips to 50% of confluence, starved for 2 hrs and treated with 1 µM MK0677 for 1 hour. In some cases, cells were pre-treated with 1 µM FR900359 or 500 nM substance P for 2 hours. Subsequently cells were fixed in 4 % PFA followed by permeabilization in 0.2% Triton X-100 and blocking in 1% FCS. After extensive washing with PBS cells were stained with a YAP/TAZ rabbit mAb (Cell Signaling Technology Cat# 8418, RRID:AB_10950494, 1:200) overnight at 4°C or 2 hrs at room temperature. After washing with PBS cells were incubated with Alexafluor 488-conjugated goat-anti rabbit (1:200), DAPI (1:50000) and Phalloidin-ATTO-647N (500 nM) for 1 hour at room temperature. Cells were then washed again with PBS before being mounted on microscope slides with ProLong Gold Antifade Mountant (Thermo Fisher Scientific).

Image analysis

In order to measure the dependency of DAPI stained nuclei and YAP/TAZ stained cells, used Image J 1.47 and a colocalization plugin. Images for each channel were background subtracted and Pearson's colocalization coefficient was calculated using the following equation:

$$R p = \frac{\sum(A_i - a) \times (B_i - b)}{\sqrt{[\sum(A_i - a)^2 \times \sum(B_i - b)^2]}}$$

The channel A and channel B grey values of voxel i are noted as A_i and B_i , respectively, and the average intensities over the full image as a and b.

RNA extraction and quantitative PCR

Before being extracted with RNA easy kit according to the manufacturer's protocol (Quiagen, Courtaboeuf, France) cells were washed with cold PBS. For reverse transcription with M-MLV (Promega) 1 µg of RNA was used. Diluted cDNA was used for real-time quantitative PCR using LightCycler® 480 SYBR Green I Master (Roche, Meylan, France), gene specific primers (see primer sequences) and the Light Cycler® 480 system (Roche, Meylan, France). GAPDH was taken as housekeeping gene for normalization purposes.

Western Blot analysis

Cells were treated and cultured as described in the previous sections. Treated cells were washed, lysed in RIPA buffer (Thermo Fisher Scientific, Ulm, Germany) and resolved using on 10% SDS-PAGE. Proteins were then transferred onto a PVDF membrane and subsequently immunoblotted with anti phospho-S127 YAP antibody (1:1000, Cell Signaling, Leiden, The Netherlands) or total YAP antibody (1:1000, Cell Signaling, Leiden, The Netherlands), for the control of G12/13 knockdown siRNA transfected cells were lysed and processed as described above for immunoblotting using an anti-G α 13 antibody (# H00010672-M01, Abnova, Taipei City, Taiwan) or an anti GAPDH antibody for control loading (G9545, SIGMA).

ERK1/2 activation

Measurement of ERK1/2 activation was performed using the Advanced ERK phospho-T202/Y204 kit (#64AERPEG, Cisbio, Codolet, France), which uses a cryptate-labeled anti-ERK monoclonal antibody and a d2-labeled anti-phospho-ERK monoclonal antibody. Cells plated in 96 well plate were stimulated with the appropriate compounds, and then the cell lysates were transferred to a 384-well plate, and both antibodies were added; the read was performed 2 h later using Pherastar (BMGLabtech) plate reader.

Data analysis

Concentration-response relationships were analyzed using Graph Pad Prism 4 (San Diego, CA, USA) by three parameter non-linear regression according to the following sigmoidal dose-response equation:

$Y = \text{Bottom} + (\text{Top} - \text{Bottom}) / (1 + 10^{((\text{LogEC50} - X)))}$, where X is the logarithm of concentration and Y is the response.

For statistical tests, where only two datasets were being compared an unpaired Student's t-test (two-tailed) was used, where $p < 0.05$ was deemed statistically significant. Where greater than two datasets were compared, one-way analysis of variance (ANOVA) tests were used with $p < 0.05$ being accepted as significantly different. ANOVA tests were followed by the Dunnett's or Tukey's multiple comparison test.

Results

Assessment of YAP S127 phosphorylation in HEK293 cells

To screen for regulatory inputs on YAP activity in cells, we developed innovative rapid and easy-to-use assays for 96 or 384 well plate formats, based on the HTRF® technology (SuppFig.1, [35], and <https://fr.cisbio.eu/>). These Phospho-YAP (S127) HTRF® and Total-YAP kits are based on a relative quantification of both the S127 phosphorylated form of YAP (P-YAP) and of total YAP (T-YAP) using a pair of antibodies labelled with time-resolved FRET (TR-FRET) compatible fluorophores. While the T-YAP assay needs the use of two anti-YAP antibodies that recognize the protein whether or not phosphorylated, the P-YAP assay is based on the use of an antibody recognizing specifically YAP phosphorylated on Ser 127, one of the major events related to YAP inhibition, and a second anti-YAP antibody (SuppFig.1A, M&M, and [35]). The signal obtained with the S127-P-YAP assay can be normalized to the signal obtained with the T-YAP assay to generate the ratio P-YAP/T-YAP (SuppFig.1A), in order to eliminate well to well cell number variation.

This assay was first validated in HEK293 cells. As previously described [25], serum 10% induced a decrease of S127-YAP phosphorylation in overnight serum-deprived cells, as similarly detected using both a western blot approach (SuppFig.1B) and the innovative P-YAP and T-YAP (and P-YAP/T-YAP ratio) HTRF® assays (SuppFig.1A) over a time course of 240 min. Actually, YAP dephosphorylation by application of serum was recorded after a serum starvation step that allows YAP re-phosphorylation. Note that YAP was getting phosphorylated back at 240 min after stimulation as detected by both approaches (SuppFig.1A & B). Interestingly, the expected increase of YAP expression due to low phosphorylation state was also detected (SuppFig.1A & B). We then used our HTRF®-based assays to assess the regulation of YAP phosphorylation by GPCRs. Yu et al. showed that the effect of serum on YAP dephosphorylation in HEK293 cells was due at least partly to the activation of S1P receptors by S1P ligand present in serum [25]. Indeed, we observed that both serum and S1P induced a decrease of YAP S127 phosphorylation in HEK293 cells after overnight serum deprivation (SuppFig.1C). The serum effect was more pronounced at 60 min and lasted longer as the effect was still present at 120 min in contrast to S1P (SuppFig.1C).

YAP S127 dephosphorylation in response to GHS-R1a stimulation

These assays were then used to assess the control of YAP phosphorylation by the GHS-R1a Ghrelin GPCR. We used the commercial HEK293 cell line #C1SU1GHSR1A (GHS-R1a HEK293 cells) stably

expressing GHS-R1a, as illustrated by Ghrelin and the agonist MK0677 displacing the binding of Ghrelin receptor Red Agonist (Perkin-Elmer/Cisbio) (SuppFig.2A & B) [34]. GHS-R1a is known to activate Gq, as well as Gi/o and G12/13 [37–39]. In GHS-R1a HEK293 cells, Ghrelin and the full GHS-R1A agonist MK0677 induced the generation of IP1-3 second messengers as measured using an HTRF® IPOne assay, in a dose-dependent manner ($pEC_{50} = 9.63 \pm 0.16$), which was completely reversed in the presence of the Gq inhibitor FR900359 (Fig.1A). This confirms that GHS-R1a activates Gq in this stable cell line. We then showed that GHS-R1a activated YAP in this cell line. Indeed, application of either the endogenous agonist Ghrelin or the synthetic agonist MK0677 resulted in a robust, dose-dependent S127 YAP dephosphorylation (Fig.1B), both displaying similar efficacy (55% for ghrelin and 49% for MK0677, respectively) and EC_{50} s ($pEC_{50} = -9.05 \pm 0.14$ and -9.54 ± 0.14 , respectively), similar to the ones determined with the IPOne assay (Fig.1A). Besides, we used the P-YAP/T-YAP ratio (Fig.1B) generated by normalizing the P-YAP data (Fig.1C) by the T-YAP protein level (Fig.1D), which were determined after overnight serum-starvation of the cells, since a weak but not significant MK0677 response was obtained in non-starved cells likely due to serum effect on YAP (Data not shown).

GHS-R1a controls YAP activity through Gq and not G12/13, in contrast to the S1P receptors

We then demonstrated that the GHS-R1a-induced YAP regulation resulted from the activation of the Gq pathway (Fig.2 and SuppFig.3). Indeed, the Gq inhibitor FR900359 [40] completely suppressed the MK0677-induced YAP dephosphorylation (Fig.2A and SuppFig.3). “In contrast, treatment with siRNAs targeting $G\alpha_{12}$ or $G\alpha_{13}$ mRNA, used either individually or pooled, did not alter the MK0677 response (Fig.2A and SuppFig.3, data not shown for individual siRNAs), although they largely decreased $G\alpha_{12}$ or $G\alpha_{13}$ mRNA expression level (Fig.2B) and $G\alpha_{13}$ G protein amount to undetectable levels (Fig.2C). In agreement, siRNA treatment did not further increase the Gq inhibitor effect (Fig.2A and SuppFig.3, data not shown for individual siRNAs).” Actually, neither the efficacy of MK0677 nor the EC_{50} s of MK0677 ($pEC_{50} = -9.48 \pm 0.21$) were affected by siRNAs against $G\alpha_{12}$ and $G\alpha_{13}$ RNAs (pEC_{50} of MK0677 = -9.38 ± 0.22), nor the control siRNAs (pEC_{50} of MK0677 = -9.43 ± 0.26). It has to be noted that the treatment of the cells by the pertussis toxin PTX (500 ng/mL) that inhibits the Gi/o G proteins did not affect the MK0677-induced YAP dephosphorylation (SuppFig.4A), although GHS-R1a was able to activate Gi/o G proteins, as illustrated by the reduction of the MK0677-induced ERK1/2 signaling upon PTX treatment (SuppFig.4B). Taken together, these data support the activation of YAP by GHS-R1a resulting exclusively from a Gq-pathway. In contrast, S1P treatment in the same cells showed that the S1P-induced YAP activity was mediated mainly by the G12/13 pathway (Fig.3A and SuppFig.5). Indeed, in cells transfected with siRNAs targeting the $G\alpha_{12}$ and $G\alpha_{13}$ RNAs to eliminate $G\alpha_{12}$ and $G\alpha_{13}$

proteins (Fig.3B), S1P-induced YAP dephosphorylation was largely reduced (Fig.3A and SuppFig.5), while treatment with control siRNAs did not modify S1P effect (Fig.3A and SuppFig.5). Interestingly, blocking at the same time the G12/13 pathway and the Gq pathway using the FR900359 compound led to a total suppression of the S1P response (Fig.3A and SuppFig.5), demonstrating that the Gq pathway also contributed to the YAP regulation by S1P receptor. Moreover, treatment with FR900359 alone increased the P-YAP/T-YAP ratio in these cells, but S1P could still dephosphorylate YAP (Fig.3A and SuppFig.5). Our data then demonstrate that agonist-activated GHS-R1a does induce YAP dephosphorylation through Gq and not G12/13 in contrast to the S1P receptors.

GHS-R1a constitutive activity induces sustained YAP dephosphorylation

Inhibiting Gq with FR900350 was found to strongly affect the basal level of P-YAP/T-YAP in GHS-R1a HEK293 cells (Fig.2A and Fig.3A) ($48.6 \% \pm 12.8\%$ SEM increase in P-YAY/T-YAY as compared to non-treated cells). Moreover, this strong reduction of YAP dephosphorylation in GHS-R1a HEK293 cells upon FR900359 treatment (Fig.2A and Fig.3A), often led to a decrease of the total YAP protein level (SuppFig.3 and SuppFig.5). These data suggested a tonic effect of Gq on YAP activity. The GHS-R1a is well-known for its high ligand-independent constitutive activity [41,42], easily detected through the constitutive activation of the Gq pathway [41]. Actually, a large decrease of the basal level of IP second messenger production was also observed upon treatment with the Gq inhibitor FR900359, as observed in Fig.1A ($25.8\% \pm 8.4\%$ SEM), indicating that FR900359 did inhibit the GHS-R1a-induced Gq constitutive activity. A further demonstration was provided by the use of two compounds, Substance P analogue (SPA) [42] and JMV5289 [33], with inverse agonist activity able to decrease the constitutive activity of GSH-R1a. Both SPA and JMV5289 induced in a dose-dependent effect a reduction of the basal production of IP second messengers in GHS-R1a HEK293 cells (Fig.4A, increase HTRF® ratio of $18.0 \pm 5.3\%$ for SPA and 14.3 ± 3.7 for JMV 5289), while the agonist MK0677 and JMV3011 compound [39,43] increased IP3 production, although to a distinct extend (Fig.4A). Indeed, we observed a very partial agonist effect of JMV3011 although it was described as an antagonist [39]. These results confirmed the presence of a strong constitutive activity of GHS-R1a toward the Gq pathway, likely at the origin of the constitutive dephosphorylation of YAP.

We then demonstrated that the constitutive dephosphorylation of YAP in the GHS-R1a HEK293 cells was due to the constitutive activity of GHS-R1a using both HTRF® and western blot approaches (Fig.4B-D and SuppFig.6). Indeed, both inverse agonists SPA and JMV5289 dose-dependently increased YAP phosphorylation by 22 % and 7 %, respectively (Fig.4B & C and SuppFig.6A). In contrast, compound JMV3011 decreased YAP phosphorylation at high concentration (Fig.4B). Further analysis revealed that

saturating concentration of SPA led to a reduced potency of MK0677 on YAP dephosphorylation ($pEC_{50} -7.47 \pm 0.22$ vs $pEC_{50} -9.59 \pm 0.17$, Fig.4D and SuppFig.6B). More interestingly, the basal YAP phosphorylation was strongly increased likely due to the inverse agonist action of SPA (1.44 ± 0.03 a.u. for SPA vs 0.98 ± 0.02 a.u. for MK0677, Fig.4D and SuppFig.6B), while the efficacy of MK0677 was slightly reduced (0.75 ± 0.07 a.u. vs 0.58 ± 0.02 a.u., Fig.4D and SuppFig.6B). Taken together, these data demonstrated that controlling the activity of GHS-R1a using agonists or inverse agonists allows a precise up and down regulation of YAP S127 phosphorylation.

GHS-R1a controls the nuclear YAP/TAZ localization and target gene expression

We then examined whether the GHS-R1a constitutive Gq activation could control YAP nuclear localization the same way as an acute GHS-R1a agonist-driven Gq stimulation. Phosphorylation of YAP on S127 by LATS1/2 is known to favor its interaction with 14-3-3 proteins resulting in cytoplasmic sequestration [44,45]. In contrast, dephosphorylation of YAP, as described also for its related partner TAZ, generally triggers its translocation to the nucleus where YAP controls its target gene expression by interacting directly with the TEAD 1-4 transcription factor family [6,21,23,46]. To investigate whether GHS-R1a not only contributes to YAP dephosphorylation but also leads to its downstream translocation to the nucleus via the Gq pathway, we studied nuclear YAP/TAZ localization by immunofluorescence microscopy (Fig.5A). Most commercially available antibodies do not discriminate between YAP and TAZ proteins, but localization of both proteins is similarly regulated in most models, although TAZ is degraded faster in the cytoplasm than YAP upon phosphorylation [47]. The overlap between nuclear staining obtained with the DAPI dye and YAP/TAZ positive immunodetection areas was calculated using the Pearson correlation coefficient to quantify YAP/TAZ nuclear localization (Fig.5B). Under basal conditions, a significant YAP/TAZ nuclear localization was observed (Fig.5A & B, $R = 0.17 \pm 0.05$). MK0677 application induced robust nuclear YAP/TAZ accumulation ($R = 0.44 \pm 0.04$). Moreover, a strong actin stress fiber formation followed through the staining of actin with dye labelled-phalloidin was observed, as often observed upon external stimuli application that control YAP activity (Fig.5A). Interestingly, treatment with the inverse agonist SPA or the Gq-inhibitor FR900359 resulted in a complete nuclear depletion of YAP/TAZ ($R = -0.066 \pm 0.06$ or $R = -0.063 \pm 0.02$ respectively) and actin polymerization was reduced when treated with SPA or absent when treated with FR900359 (Fig.5A & B). Moreover, pre-treatment of the cells with the Gq inhibitor FR900359 completely abolished the MK0677-induced YAP/TAZ nuclear translocation ($R = -0.034 \pm 0.04$), and SPA reduced it partially when tested at a sub-maximal concentration of 500 nM ($R = 0.27 \pm 0.03$) (Fig.5A & B). Taken together, these data show that a basal tonic nuclear localization of YAP/TAZ was induced by the Gq-mediated constitutive activity

of the GHS-R1a receptor, and that controlling GHS-R1a activity by agonist and inverse agonist also results in a dual up- or down-impact on YAP/TAZ nuclear translocation.

We next demonstrated that YAP dephosphorylation and nuclear translocation in response to tuning of GHS-R1a activity could also trigger dual regulation of YAP target genes expression level. When assaying by real-time PCR the mRNA expression of two of the YAP/TAZ target genes, *CTGF* and *CYR61* [23,30], an upregulation of their expression was observed in an agonist MK0677-dependent manner (Fig.6). Inversely, FR900359, and in a lesser extend SPA at sub-saturating concentration, reduced the basal expression level of both target gene mRNAs (Fig.6), indicating the presence of a constitutive expression of these two genes due to Gq constitutive activation by GHS-R1a. Thus, *CTGF* and *CYR61* YAP target gene mRNA levels can be up or down regulated depending the action of agonists or inverse agonists of GHS-R1a, in a Gq-dependent manner.

Rho pathway is involved in regulation of YAP phosphorylation by GHS-R1a

Previous studies identified Rho GTPases as essential for cytoskeletal rearrangements and stress fiber formation being involved in YAP regulation [48,49]. Thus, we investigated the role of endogenous Rho signaling in YAP regulation by inhibiting Rho GTPases with botulinum toxin C3. Treatment with toxin C3 strongly increased the basal level of the P-YAP/T-YAP ratio (Fig.7A and SuppFig.7), demonstrating the tonic activation of the Rho cascade. This effect is well detected considering the ratio P-YAP/T-YAP (Fig.7A). Indeed, the weak impact of C3 treatment detected on P-YAP signal (SuppFig.7) is likely due to the constant degradation of phosphorylated YAP leaving the nucleus, which then leads to a strong decrease of T-YAP amount as observed in SuppFig.7. The MK0677-induced effect was also reduced although not completely blocked (Fig.7B). The Rho inhibitor C3 abolished basal nuclear YAP localization and suppressed MK0677-induced YAP nuclear translocation (Fig.8A & B). Stress fiber formation in response to GHS-R1a constitutive or agonist-induced activation was largely abolished when cells were pre-treated with C3 (Fig.8A). These data suggest that the Rho pathway is mobilized up- and down by both the constitutive activity and the agonist-induced activity of GHS-R1a.

Discussion

The Hippo-YAP pathway plays a crucial role in tissues development, healing, but also in tumorigenesis processes. There are numerous molecular mechanisms allowing extracellular signals to control this pathway, but not all clearly identified. It was recently shown that GPCRs can indeed activate YAP activity through G12/13 heterotrimeric G proteins. Here, we showed that the GPCR-mediated Gq pathway can also increase YAP activity, without any contribution of either G12/13 or Gi/o proteins. Moreover, we show that by targeting a GPCR with a significant Gq constitutive coupling, it is possible to either inhibit or increase YAP activity with inverse agonists or agonists, respectively. Our data illustrate how a Gq-coupled GPCR can act as a molecular switch to finely tune up or down YAP activity.

In order to be able to screen for conditions and drugs, we developed innovative and efficient assays, based on the HTRF® technology allowing the relative quantification of total YAP and S127 phosphorylated YAP protein [35]. Using a stable HEK293 cell line expressing the GHS-R1a receptor, we show that two different GPCRs activate YAP through two distinct pathways. Indeed, activation of the S1P receptor induced S127 YAP dephosphorylation mainly through the mobilization of G12/13 pathway, while the GHS-R1a receptor also dephosphorylates YAP but through the Gq pathway exclusively. Moreover, we showed that the downstream YAP cascade events, like the nuclear YAP localization and the YAP-regulated gene expression, induced by GHS-R1a stimulation were abolished when the Gq pathway was inhibited. These data reveal that two different receptors can control S127 YAP dephosphorylation/activation using different G protein pathways in the same cells.

It was previously reported that activation of YAP by the M3 Acetylcholine receptor in gastric tumor or TMK-1 cells involves Gq as their effect on YAP activity was inhibited by the Gq inhibitor YM254890 [50,51]. YM254890 treatment by itself strongly increased the basal YAP phosphorylation, making the quantification of the M3 agonist effect difficult to analyze and may occlude the M3-mediated inhibition. Moreover, in AGS cells expressing M3, the transfection of the control plasmid already induced a decrease in YAP activity, suggesting that the Hippo pathway is reacting to cell transfection. At last, it was not possible to determine whether another pathway could also be involved, as there was no use of M3 antagonist to compare with the action of the Gq inhibitor, nor of inhibitors of other G protein subtypes (G12/13 or Gi/o). The estrogen GPCR (GPER) also activates YAP in breast cancer cells through Gq, but the inhibition of the activity of the different players of the YAP cascade was not quantified and may not be total. Eventually, the G12/13 involvement was not addressed either [52]. In contrast, the use of siRNA against G α 12/13 that strongly reduced the YAP activation by S1P in the GHS-R1a stable HEK3293 cells but not that induced by GHS-R1a activation, indicated that G12/13 were not required for GHS-R1a to

induced YAP dephosphorylation. Yu et al. [25] reported that mutated $G_{\alpha i/o}$ G proteins were also able to induce YAP activation. In our hands, there is no contribution of these G proteins in the GHS-R1a YAP response, as treatment with the $G_{i/o}$ protein inhibitor PTX toxin did not block MK0677-mediated YAP activation. Taken together, these results point out that different G protein pathways and even distinct combinations of them can control YAP activity, ranging from a pure Gq or G12/13 activation to the combination of G12/13, Gq, and $G_{i/o}$ pathways, even in a given cell. Specific combinations of receptors and G proteins in a given cell will then be determinant regarding the pathways mobilized for controlling YAP activity by GPCRs.

Gq-mediated activation of YAP has been observed in uveal melanomas and blue nevi cancer cells [53], in which mutations in the *GNAQ* and *GN11* genes have been shown to generate constitutively active $G_{\alpha q}$ and $G_{\alpha 11}$ proteins resulting in tumorigenesis processes. Most mutations occurred in the ras-like domain of $G_{\alpha q}$ or $G_{\alpha 11}$ [53,54] making them unable to hydrolyze GTP, resulting in a strong constitutive activity that turns *GNAQ/11* into oncogenes. These constitutively active G proteins constantly drive the activation of YAP. Indeed, activated FAK phosphorylates MOB1 that is then no more able to interact with and inhibit YAP. Interestingly, Yu et al. reported that mutations engineered to stabilize Gq/11 or $G_{i/o}$ α subunits in a constitutively activated state also lead to an increased YAP activity when transfected in HEK293 cells, independently of GPCR [25]. However, the signaling pathways involved have not been assessed, nor whether a GPCR could mimic such an effect. Our results showed that Gq itself can control YAP activity when acutely and also when constantly activated by the native constitutive activity of a GPCRs. This means that there is no need of a constitutive mutation of the Gq protein to gain YAP activation. However, the signaling pathway mobilized by the acute GPCR-induced Gq activation, the engineered mutated Gq/11, or the pathologic mutation of *GNAQ* or *GN11* in melanomas, could be different. This is an intriguing issue to consider that constitutively active G proteins could behave and signal into the cells a different way than acutely activated G proteins. G protein long-term activity may promote a change in partner association or distribution such that the signaling cascade down the Gq protein is different. An intriguing issue has been observed in melanoma cells, where the pathologic action of the mutated Gq or G11 proteins result from their atypical association to the protein Trio and not from activation of their canonical PLC partner [55]. Trio protein regulates the Rho pathway that controls YAP activity via the FAK protein [56]. This is reminiscent of constitutive mGlu5 glutamate GPCRs that couples differently to its signaling partners and promotes distinct cellular responses when their activation is induced by their ligand or driven by their own natural constitutive activity [57].

By analyzing YAP phosphorylation, YAP/TAZ nuclear localization, and target gene expression, we demonstrate that a GPCR is able to impact on Hippo pathway activation in absence of its ligand, thanks to its intrinsic constitutive activity. Indeed, GHS-R1a displays a high constitutive activity resulting in a constant activation of Gq [41,42] (Fig.1 & 4). Thus, inverse agonists, like SPA, which inhibit the GHS-R1a constitutive activity and its associated downstream Gq signaling cascade, also inhibits the basal YAP activation (Fig.4). This means one can either increase or decrease YAP activity depending on the ligand used, agonists or inverse agonist, resulting in a fine up- or down-regulation of YAP activity through a pure Gq pathway. To our knowledge, this is the first time a basal activation of YAP is described resulting from the constitutive activity of a GPCR, and then inhibited by inverse agonist. As many GPCRs display constitutive activity at various extends, it would be interesting to explore whether they also impact the basal YAP activity in physiological models and more interestingly in pathological conditions like in cancer cells.

We have identified the GHS-R1a receptor as a molecular switch that induces both constitutive and ligand-induced acute nuclear YAP activation and target gene expression. These results establish signaling mechanisms by which GHS-R1a activates YAP and further triggers the YAP signaling axis down to gene expression regulation. The link between GHS-R1a and the YAP/TAZ signaling axis might have several essential implications. The ghrelin receptor is mainly expressed in the hypothalamus and the gastrointestinal tract and is involved in a broad range of physiological functions [58]. Ghrelin is known to drive proliferation and differentiation and inhibiting apoptosis in several cellular models [59–61]. While several studies suggest that Ghrelin promotes cancer such as colorectal malignancies [62] or renal cell carcinoma metastasis [63], neither Ghrelin nor Anamorelin, used as GHS-R1a agonist for treatment of cancer cachexia encouraged tumor growth in xenograft models [64] or in humans with NSLC (non-small lung cell carcinoma) in a short-term phase 3 safety extension study [65]. Current literature is still controversial regarding the contribution of Ghrelin and its receptor to cancer [66]. Long term studies of Ghrelin effects on cancer progression as well as deciphering Ghrelin receptor expression patterns in cancer would shed more lights on the role of Ghrelin in tumorigenesis.

Funding

This work was supported by the Labex EpiGenMed, an « Investissements d'avenir » program of the French government (reference ANR-10-LABX-12-01) to JPP, the Fondation Recherche Médicale (FRM DEQ20170336747) to JPP, and by the EIDOS Collaborative team IGF-Cisbio (Codolet, France). DZ was supported by a Grant from the Région Occitanie (France).

References

1. Dong J, Feldmann G, Huang J, Wu S, Zhang N, Comerford SA, Gayyed MF, Anders RA, Maitra A, Pan D (2007) Elucidation of a Universal Size-Control Mechanism in Drosophila and Mammals. *Cell* **130**: 1120–1133.
2. Totaro A, Panciera T, Piccolo S (2018) YAP/TAZ upstream signals and downstream responses. *Nat Cell Biol* **20**: 888–899.
3. Yin F, Yu J, Zheng Y, Chen Q, Zhang N, Pan D (2013) Spatial organization of Hippo signaling at the plasma membrane mediated by the tumor suppressor Merlin/NF2. *Cell* **154**: 1342–1355.
4. Hong W, Guan K-L (2012) The YAP and TAZ transcription co-activators: key downstream effectors of the mammalian Hippo pathway. *Semin Cell Dev Biol* **23**: 785–793.
5. Lei Q-Y, Zhang H, Zhao B, Zha Z-Y, Bai F, Pei X-H, Zhao S, Xiong Y, Guan K-L (2008) TAZ promotes cell proliferation and epithelial-mesenchymal transition and is inhibited by the hippo pathway. *Mol Cell Biol* **28**: 2426–2436.
6. Zhao B, Ye X, Yu J, Li L, Li W, Li S, Yu J, Lin JD, Wang C-Y, Chinnaiyan AM, et al. (2008) TEAD mediates YAP-dependent gene induction and growth control. *Genes Dev* **22**: 1962–1971.
7. Johnson R, Halder G (2014) The two faces of Hippo: targeting the Hippo pathway for regenerative medicine and cancer treatment. *Nat Rev Drug Discov* **13**: 63–79.
8. Liu H, Du S, Lei T, Wang H, He X, Tong R, Wang Y (2018) Multifaceted regulation and functions of YAP/TAZ in tumors (Review). *Oncol Rep* **40**: 16–28.
9. Luo J, Yu F-X (2019) GPCR-Hippo Signaling in Cancer. *Cells* **8**:
10. Zanconato F, Cordenonsi M, Piccolo S (2016) YAP/TAZ at the Roots of Cancer. *Cancer Cell* **29**: 783–803.
11. Hiemer SE, Szymaniak AD, Varelas X (2014) The transcriptional regulators TAZ and YAP direct transforming growth factor β -induced tumorigenic phenotypes in breast cancer cells. *J Biol Chem* **289**: 13461–13474.
12. Nallet-Staub F, Marsaud V, Li L, Gilbert C, Dodier S, Bataille V, Sudol M, Herlyn M, Mauviel A (2014) Pro-invasive activity of the Hippo pathway effectors YAP and TAZ in cutaneous melanoma. *J Invest Dermatol* **134**: 123–132.

13. Wang L, Shi S, Guo Z, Zhang X, Han S, Yang A, Wen W, Zhu Q (2013) Overexpression of YAP and TAZ is an independent predictor of prognosis in colorectal cancer and related to the proliferation and metastasis of colon cancer cells. *PloS One* **8**: e65539.
14. Xia Y, Zhang Y-L, Yu C, Chang T, Fan H-Y (2014) YAP/TEAD co-activator regulated pluripotency and chemoresistance in ovarian cancer initiated cells. *PloS One* **9**: e109575.
15. Bartucci M, Dattilo R, Moriconi C, Pagliuca A, Mottolose M, Federici G, Benedetto AD, Todaro M, Stassi G, Sperati F, et al. (2015) TAZ is required for metastatic activity and chemoresistance of breast cancer stem cells. *Oncogene* **34**: 681–690.
16. Cordenonsi M, Zanconato F, Azzolin L, Forcato M, Rosato A, Frasson C, Inui M, Montagner M, Parenti AR, Poletti A, et al. (2011) The Hippo transducer TAZ confers cancer stem cell-related traits on breast cancer cells. *Cell* **147**: 759–772.
17. Mo J-S, Park HW, Guan K-L (2014) The Hippo signaling pathway in stem cell biology and cancer. *EMBO Rep* **15**: 642–656.
18. Koo JH, Guan K-L (2018) Interplay between YAP/TAZ and Metabolism. *Cell Metab* **28**: 196–206.
19. Mo J-S, Meng Z, Kim YC, Park HW, Hansen CG, Kim S, Lim D-S, Guan K-L (2015) Cellular energy stress induces AMPK-mediated regulation of YAP and the Hippo pathway. *Nat Cell Biol* **17**: 500–510.
20. Mo J-S (2017) The role of extracellular biophysical cues in modulating the Hippo-YAP pathway. *BMB Rep* **50**: 71–78.
21. Zhao B, Wei X, Li W, Udan RS, Yang Q, Kim J, Xie J, Ikenoue T, Yu J, Li L, et al. (2007) Inactivation of YAP oncoprotein by the Hippo pathway is involved in cell contact inhibition and tissue growth control. *Genes Dev* **21**: 2747–2761.
22. Yang C-C, Graves HK, Moya IM, Tao C, Hamaratoglu F, Gladden AB, Halder G (2015) Differential regulation of the Hippo pathway by adherens junctions and apical-basal cell polarity modules. *Proc Natl Acad Sci U S A* **112**: 1785–1790.
23. Dupont S, Morsut L, Aragona M, Enzo E, Giulitti S, Cordenonsi M, Zanconato F, Le Digabel J, Forcato M, Bicciato S, et al. (2011) Role of YAP/TAZ in mechanotransduction. *Nature* **474**: 179–183.
24. Hansen CG, Moroishi T, Guan K-L (2015) YAP and TAZ: a nexus for Hippo signaling and beyond. *Trends Cell Biol* **25**: 499–513.

25. Yu F-X, Zhao B, Panupinthu N, Jewell JL, Lian I, Wang LH, Zhao J, Yuan H, Tumaneng K, Li H, et al. (2012) Regulation of the Hippo-YAP pathway by G-protein-coupled receptor signaling. *Cell* **150**: 780–791.
26. Feng X, Liu P, Zhou X, Li M-T, Li F-L, Wang Z, Meng Z, Sun Y-P, Yu Y, Xiong Y, et al. (2016) Thromboxane A2 Activates YAP/TAZ Protein to Induce Vascular Smooth Muscle Cell Proliferation and Migration. *J Biol Chem* **291**: 18947–18958.
27. Miller E, Yang J, DeRan M, Wu C, Su AI, Bonamy GMC, Liu J, Peters EC, Wu X (2012) Identification of serum-derived sphingosine-1-phosphate as a small molecule regulator of YAP. *Chem Biol* **19**: 955–962.
28. Iglesias-Bartolome R, Torres D, Marone R, Feng X, Martin D, Simaan M, Chen M, Weinstein LS, Taylor SS, Molinolo AA, et al. (2015) Inactivation of a G α (s)-PKA tumour suppressor pathway in skin stem cells initiates basal-cell carcinogenesis. *Nat Cell Biol* **17**: 793–803.
29. Hot B, Valnohova J, Arthofer E, Simon K, Shin J, Uhlén M, Kostenis E, Mulder J, Schulte G (2017) FZD10-G α 13 signalling axis points to a role of FZD10 in CNS angiogenesis. *Cell Signal* **32**: 93–103.
30. Mo J-S, Yu F-X, Gong R, Brown JH, Guan K-L (2012) Regulation of the Hippo-YAP pathway by protease-activated receptors (PARs). *Genes Dev* **26**: 2138–2143.
31. Wang J, Sinnott-Smith J, Stevens JV, Young SH, Rozengurt E (2016) Biphasic Regulation of Yes-associated Protein (YAP) Cellular Localization, Phosphorylation, and Activity by G Protein-coupled Receptor Agonists in Intestinal Epithelial Cells: A NOVEL ROLE FOR PROTEIN KINASE D (PKD). *J Biol Chem* **291**: 17988–18005.
32. Zhu H, Cheng X, Niu X, Zhang Y, Guan J, Liu X, Tao S, Wang Y, Zhang C (2015) Proton-sensing GPCR-YAP Signalling Promotes Cell Proliferation and Survival. *Int J Biol Sci* **11**: 1181–1189.
33. Els S, Schild E, Petersen PS, Kilian T-M, Mokrosinski J, Frimurer TM, Chollet C, Schwartz TW, Holst B, Beck-Sickinger AG (2012) An aromatic region to induce a switch between agonism and inverse agonism at the ghrelin receptor. *J Med Chem* **55**: 7437–7449.
34. M’Kadmi C, Cabral A, Barrile F, Giribaldi J, Cantel S, Damian M, Mary S, Denoyelle S, Dutertre S, Péraldi-Roux S, et al. (2019) N-Terminal Liver-Expressed Antimicrobial Peptide 2 (LEAP2) Region Exhibits Inverse Agonist Activity toward the Ghrelin Receptor. *J Med Chem* **62**: 965–973.
35. Zindel D, Vol C, Lecha O, Bequignon I, Bilgic M, Vereecke M, Charrier-Savournin F, Romier M, Trinquet E, Pin J-P, et al. (2019) HTRF® Total and Phospho-YAP (Ser127) Cellular Assays.

Methods Mol Biol Clifton NJ **1893**: 153–166.

36. Brulé C, Perzo N, Joubert J-E, Sainsily X, Leduc R, Castel H, Prézeau L (2014) Biased signaling regulates the pleiotropic effects of the urotensin II receptor to modulate its cellular behaviors. *FASEB J Off Publ Fed Am Soc Exp Biol* **28**: 5148–5162.
37. Camiña JP, Lodeiro M, Ischenko O, Martini AC, Casanueva FF (2007) Stimulation by ghrelin of p42/p44 mitogen-activated protein kinase through the GHS-R1a receptor: role of G-proteins and beta-arrestins. *J Cell Physiol* **213**: 187–200.
38. Damian M, Mary S, Maingot M, M’Kadmi C, Gagne D, Leyris J-P, Denoyelle S, Gaibelet G, Gavara L, Garcia de Souza Costa M, et al. (2015) Ghrelin receptor conformational dynamics regulate the transition from a preassembled to an active receptor:Gq complex. *Proc Natl Acad Sci U S A* **112**: 1601–1606.
39. M’Kadmi C, Leyris J-P, Onfroy L, Galés C, Saulière A, Gagne D, Damian M, Mary S, Maingot M, Denoyelle S, et al. (2015) Agonism, Antagonism, and Inverse Agonism Bias at the Ghrelin Receptor Signaling. *J Biol Chem* **290**: 27021–27039.
40. Schrage R, Schmitz A-L, Gaffal E, Annala S, Kehraus S, Wenzel D, Büllsbach KM, Bald T, Inoue A, Shinjo Y, et al. (2015) The experimental power of FR900359 to study Gq-regulated biological processes. *Nat Commun* **6**: 10156.
41. Damian M, Marie J, Leyris J-P, Fehrentz J-A, Verdié P, Martinez J, Banères J-L, Mary S (2012) High constitutive activity is an intrinsic feature of ghrelin receptor protein: a study with a functional monomeric GHS-R1a receptor reconstituted in lipid discs. *J Biol Chem* **287**: 3630–3641.
42. Holst B, Cygankiewicz A, Jensen TH, Ankersen M, Schwartz TW (2003) High constitutive signaling of the ghrelin receptor--identification of a potent inverse agonist. *Mol Endocrinol Baltim Md* **17**: 2201–2210.
43. Moulin A, Demange L, Ryan J, Mousseaux D, Sanchez P, Bergé G, Gagne D, Perrissoud D, Locatelli V, Torsello A, et al. (2008) New trisubstituted 1,2,4-triazole derivatives as potent ghrelin receptor antagonists. 3. Synthesis and pharmacological in vitro and in vivo evaluations. *J Med Chem* **51**: 689–693.
44. Hao Y, Chun A, Cheung K, Rashidi B, Yang X (2008) Tumor Suppressor LATS1 Is a Negative Regulator of Oncogene YAP. *J Biol Chem* **283**: 5496–5509.
45. Yu F-X, Guan K-L (2013) The Hippo pathway: regulators and regulations. *Genes Dev* **27**: 355–371.

46. Li Z, Zhao B, Wang P, Chen F, Dong Z, Yang H, Guan K-L, Xu Y (2010) Structural insights into the YAP and TEAD complex. *Genes Dev* **24**: 235–240.
47. Finch-Edmondson ML, Strauss RP, Passman AM, Sudol M, Yeoh GC, Callus BA (2015) TAZ Protein Accumulation Is Negatively Regulated by YAP Abundance in Mammalian Cells. *J Biol Chem* **290**: 27928–27938.
48. Ridley AJ, Hall A (1992) The small GTP-binding protein rho regulates the assembly of focal adhesions and actin stress fibers in response to growth factors. *Cell* **70**: 389–399.
49. Spiering D, Hodgson L (2011) Dynamics of the Rho-family small GTPases in actin regulation and motility. *Cell Adhes Migr* **5**: 170–180.
50. Gong R, Hong AW, Plouffe SW, Zhao B, Liu G, Yu F-X, Xu Y, Guan K-L (2015) Opposing roles of conventional and novel PKC isoforms in Hippo-YAP pathway regulation. *Cell Res* **25**: 985–988.
51. Hayakawa Y, Sakitani K, Konishi M, Asfaha S, Niikura R, Tomita H, Renz BW, Tailor Y, Macchini M, Middelhoff M, et al. (2017) Nerve Growth Factor Promotes Gastric Tumorigenesis through Aberrant Cholinergic Signaling. *Cancer Cell* **31**: 21–34.
52. Zhou X, Wang S, Wang Z, Feng X, Liu P, Lv X-B, Li F, Yu F-X, Sun Y, Yuan H, et al. (2015) Estrogen regulates Hippo signaling via GPER in breast cancer. *J Clin Invest* **125**: 2123–2135.
53. Van Raamsdonk CD, Bezrookove V, Green G, Bauer J, Gaugler L, O'Brien JM, Simpson EM, Barsh GS, Bastian BC (2009) Frequent somatic mutations of GNAQ in uveal melanoma and blue naevi. *Nature* **457**: 599–602.
54. Van Raamsdonk CD, Griewank KG, Crosby MB, Garrido MC, Vemula S, Wiesner T, Obenaus AC, Wackernagel W, Green G, Bouvier N, et al. (2010) Mutations in GNA11 in uveal melanoma. *N Engl J Med* **363**: 2191–2199.
55. Feng X, Degese MS, Iglesias-Bartolome R, Vaque JP, Molinolo AA, Rodrigues M, Zaidi MR, Ksander BR, Merlino G, Sodhi A, et al. (2014) Hippo-independent activation of YAP by the GNAQ uveal melanoma oncogene through a trio-regulated rho GTPase signaling circuitry. *Cancer Cell* **25**: 831–845.
56. Feng X, Arang N, Rigracciolo DC, Lee JS, Yeerna H, Wang Z, Lubrano S, Kishore A, Pachter JA, König GM, et al. (2019) A Platform of Synthetic Lethal Gene Interaction Networks Reveals that the GNAQ Uveal Melanoma Oncogene Controls the Hippo Pathway through FAK. *Cancer Cell* **35**: 457–472.e5.

57. Ango F, Albani-Torregrossa S, Joly C, Robbe D, Michel JM, Pin JP, Bockaert J, Fagni L (1999) A simple method to transfer plasmid DNA into neuronal primary cultures: functional expression of the mGlu5 receptor in cerebellar granule cells. *Neuropharmacology* **38**: 793–803.
58. Davenport AP, Bonner TI, Foord SM, Harmar AJ, Neubig RR, Pin J-P, Spedding M, Kojima M, Kangawa K (2005) International Union of Pharmacology. LVI. Ghrelin receptor nomenclature, distribution, and function. *Pharmacol Rev* **57**: 541–546.
59. Kim SW, Her SJ, Park SJ, Kim D, Park KS, Lee HK, Han BH, Kim MS, Shin CS, Kim SY (2005) Ghrelin stimulates proliferation and differentiation and inhibits apoptosis in osteoblastic MC3T3-E1 cells. *Bone* **37**: 359–369.
60. Lee JH, Patel K, Tae HJ, Lustig A, Kim JW, Mattson MP, Taub DD (2014) Ghrelin augments murine T-cell proliferation by activation of the phosphatidylinositol-3-kinase, extracellular signal-regulated kinase and protein kinase C signaling pathways. *FEBS Lett* **588**: 4708–4719.
61. Wang Q, Zheng M, Yin Y, Zhang W (2018) Ghrelin Stimulates Hepatocyte Proliferation via Regulating Cell Cycle Through GSK3 β /B-Catenin Signaling Pathway. *Cell Physiol Biochem Int J Exp Cell Physiol Biochem Pharmacol* **50**: 1698–1710.
62. Waseem T, Javaid-ur-Rehman, Ahmad F, Azam M, Qureshi MA (2008) Role of ghrelin axis in colorectal cancer: A novel association. *Peptides* **29**: 1369–1376.
63. Lin T-C, Liu Y-P, Chan Y-C, Su C-Y, Lin Y-F, Hsu S-L, Yang C-S, Hsiao M (2015) Ghrelin promotes renal cell carcinoma metastasis via Snail activation and is associated with poor prognosis. *J Pathol* **237**: 50–61.
64. Northrup R, Kuroda K, Duus EM, Barnes SR, Cheatham L, Wiley T, Pietra C (2013) Effect of ghrelin and anamorelin (ONO-7643), a selective ghrelin receptor agonist, on tumor growth in a lung cancer mouse xenograft model. *Support Care Cancer Off J Multinatl Assoc Support Care Cancer* **21**: 2409–2415.
65. Currow D, Temel JS, Abernethy A, Milanowski J, Friend J, Fearon KC (2017) ROMANA 3: a phase 3 safety extension study of anamorelin in advanced non-small-cell lung cancer (NSCLC) patients with cachexia. *Ann Oncol* **28**: 1949–1956.
66. Soleyman-Jahi S, Sadeghi F, Pastaki Khoshbin A, Khani L, Roosta V, Zendehdel K (2019) Attribution of Ghrelin to Cancer; Attempts to Unravel an Apparent Controversy. *Front Oncol* **9**.

Legend to figures

Figure 1: Ligand-induced activation of GHS-R1a leads to Inositol phosphate second messenger production and YAP dephosphorylation. **A** Application of the GHS-R1a receptor agonist MK0677 or Ghrelin on GHS-R1a HEK293 cells leads to the production of inositol phosphate second messengers measured through the use of the IP-One-Gq kit (Cisbio, Codolet, France). Data are the mean \pm SEM of three experiments performed in triplicates. **B-D** Application of the GHS-R1a receptor agonist MK0677 or Ghrelin on overnight serum starved GHS-R1a HEK293 cells leads to dephosphorylation of YAP Ser 127 measured through the P-YAP/T-YAP ratio (**B**). This ratio is generated by dividing the values obtained with the P-YAP assay (**C**) by those obtained with the T-YAP assay (**D**) (see M&M, Perkin-Elmer/Cisbio, Codolet, France). Data are the mean \pm SEM of three experiments performed in triplicates.

Figure 2: GHS-R1a stimulation induces YAP S127 dephosphorylation through Gq independently of G12/13. **A** GHS-R1a HEK293 cells were transfected or not (nt) with siRNAs targeting $G\alpha_{12/13}$ (si $G\alpha_{12/13}$), or with control siRNAs (Ctr siRNA). One day later, the agonist MK0677 was applied at various concentrations for 30 min at 37°C on overnight serum starved cells pretreated or not with the Gq inhibitor FR900359 (1 μ M) for 1 hour at 37°C. Cells were lysed and assessed for dephosphorylation of YAP Ser 127 measured through the P-YAP/T-YAP ratio. Results are the mean \pm SEM of three independent experiments performed in triplicates. **B-C** Knockdown of $G\alpha_{12/13}$ mRNAs (GNA12 and GNA13) and $G\alpha_{13}$ proteins in the GHS-R1a HEK293 cells, by pooled or individual siRNAs targeting $G\alpha_{12}$ or 13, was confirmed using qPCR (mean of 3 experiments, **B**) and western blot (data are representative of 3 independent experiments, **C**), techniques, respectively. Cells were treated for one day before extraction of the mRNAs and amplification using appropriate siRNAs oligonucleotides (**B**), or before analysis of the proteins in SDS-PAGE electrophoresis and western blotting with a specific anti $G\alpha_{13}$ antibody (M&M), while an anti GAPDH antibody was used for control loading (**C**).

Figure 3: S1P triggers YAP dephosphorylation on S127 through both $G\alpha_{12/13}$ and $G\alpha_q$ pathways in GHS-R1a HEK293 cells. **A** GHS-R1a HEK293 cells transfected or not (nt) with siRNA control (Ctr siRNA) or targeting $G\alpha_{12/13}$ (si $G\alpha_{12/13}$) were starved overnight and pretreated or not with 1 μ M FR900359 for 1 hour at 37°C and then stimulated with S1P for 30 min at 37°C. Subsequently, cells were lysed and analyzed for dephosphorylation of YAP Ser 127 measured through the P-YAP/T-YAP ratio. Results are the mean \pm SEM of at least 3 independent experiments. (**B**) Knockdown of $G\alpha_{13}$ protein was confirmed by western blotting with a specific anti $G\alpha_{13}$ antibody (M&M), while an anti GAPDH antibody was used for control loading (**C**).

Figure 4: GHS-R1a dual control of YAP S127 phosphorylation through both agonist-induced and agonist-independent activity. **A** Inositol phosphate second messenger production is measured with the IPOne kit (Perkin-Elmer/Cisbio, Codolet, France), in response to application of GHS-R1A agonists Ghrelin and MK0677, JMV3011, and inverse agonists SPA and JMV5289, in GHS-R1a HEK293 cells. Compounds were applied for 30 min at 37°. Results are the mean \pm SEM of three independent experiments performed in triplicates. **B** Concentration-response effects of Ghrelin, MK0677, JMV3011, SPA and JMV5289 on the P-YAP/T-YAP ratio determined in overnight serum starved GHS-R1a HEK293 cells. Compounds were applied for 30 min at 37°. Results are the mean \pm SEM of three independent experiments performed in triplicates. **C** Western blot analysis of the effect of MK0677 (1 μ M), FR900359 (1 μ M), or SPA (10 μ M), or a combination of MK0677 with either FR900359 or SPA, on total YAP and S127 YAP phosphorylation. Data are representative of 3 independent experiments. **D** Competitive inhibition of MK0677 effect by the antagonist SPA (10 μ M) measured with the P-YAP/T-YAP ratio in GHS-R1a HEK293 cells. Results are the mean \pm SEM of 3 independent experiments.

Figure 5: Opposite YAP/TAZ localization in response to GHS-R1a agonists and inverse agonist action. **A** Starved GHS-R1a HEK293 cells treated or not with MK0677 (1 μ M), FR900359 (1 μ M), or substance P (500 nM), or the indicated combination of these drugs, for 1 hour at 37°C before fixation in 4% PFA. Nuclei are labeled with DAPI (*first column panels*), YAP/TAZ localization was analyzed by immunofluorescence staining (*second column panels*), and F-actin was stained with Phalloidin (*third column panels*), and overlay was generated from staining of both DAPI and YAP/TAZ panels (*forth column panels*). The images are representatives of three independent experiments. **B** Colocalization of DAPI and YAP/TAZ labeled nuclei was determined by Pearson's overlap coefficient, R=1 YAP in nuclei, R=-1 YAP in cytoplasm. Statistics have been performed using ANOVA, followed by Bonferroni's multiple comparison test.

Figure.6: GHS-R1a-induced dual control of YAP-regulated target gene expression. Real time PCR was performed to detect mRNAs coding for CTGF and CYR61 proteins in overnight serum-starved GHS-R1a HEK293 cells treated with substance P (1 μ M) or FR900359 (1 μ M) for 5 hours or with MK0677 (1 μ M) for 4 hours. Data represent the mean \pm SEM from 4 to 5 independent experiments. Statistics were performed by one-way ANOVA followed by Dunnett's multiple comparison test.

Figure 7: MK0677-induced YAP dephosphorylation involves Rho pathway. **A** The effect of MK0677 on P-YAP/T-YAP ratio was determined in GHS-R1a HEK293 cells serum starved overnight and treated or not with 2 μ g/ml botulinum toxin C3. Data represent the mean \pm SEM from three independent experiments. **B** Percentage of MK0677-induced P-YAP/T-YAP ratio decrease in the presence or absence

of the C3 toxin. Data represent the mean \pm SEM from 3 independent experiments. Statistical analysis was performed using Student t-test.

Figure 8: YAP/TAZ nuclear localization regulation by GHS-R1a involves the Rho pathway. **A** The localization of YAP/TAZ was analyzed in GHS-R1a HEK293 cells starved overnight, pre-treated or not with 2 μ g/ml botulinum toxin C3, and then incubated with MK0677 (1 μ M) for 1 hour at 37°C before fixation in 4% PFA. Nuclei are labeled with DAPI (*first column panels*), YAP/TAZ localization was analyzed by immunofluorescence staining (*second column panels*), and F-actin was stained with Phalloidin (*third column panels*), and overlay was generated from staining of both DAPI and YAP/TAZ panels (*forth column panels*). The images are representatives of three independent experiments. **B** Colocalization of DAPI and YAP/TAZ labeled nuclei was determined by Pearson's overlap coefficient, $R=1$ YAP in nuclei, $R=-1$ YAP in cytoplasm. Statistics have been performed using ANOVA, followed by Bonferroni's multiple comparison test.

Figure 1

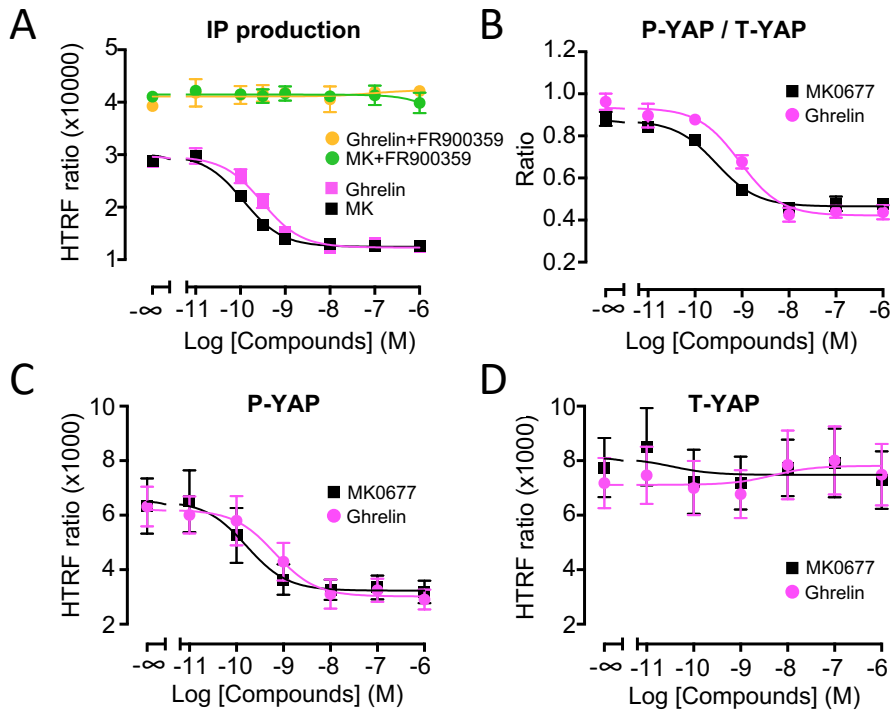


Figure 1

Figure 2

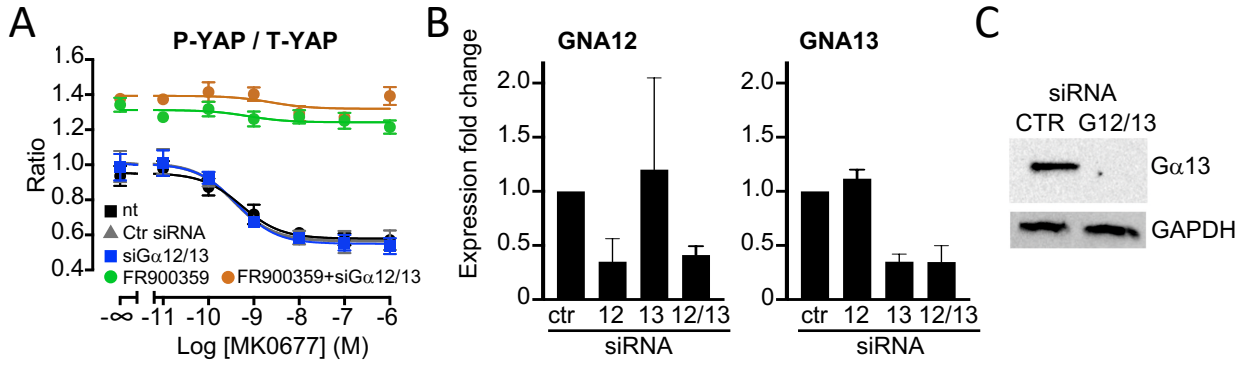


Figure 2

Figure 3

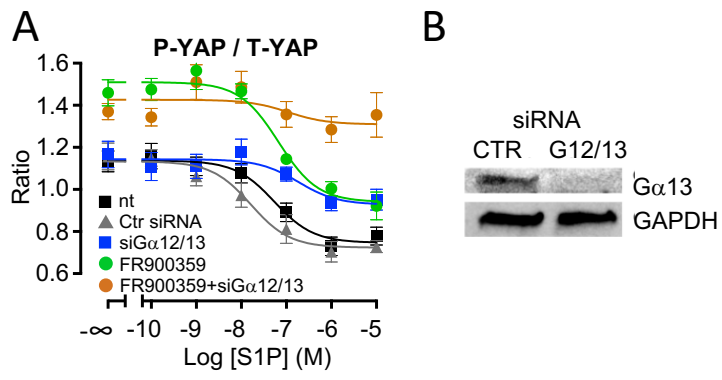


Figure 3

Figure 4

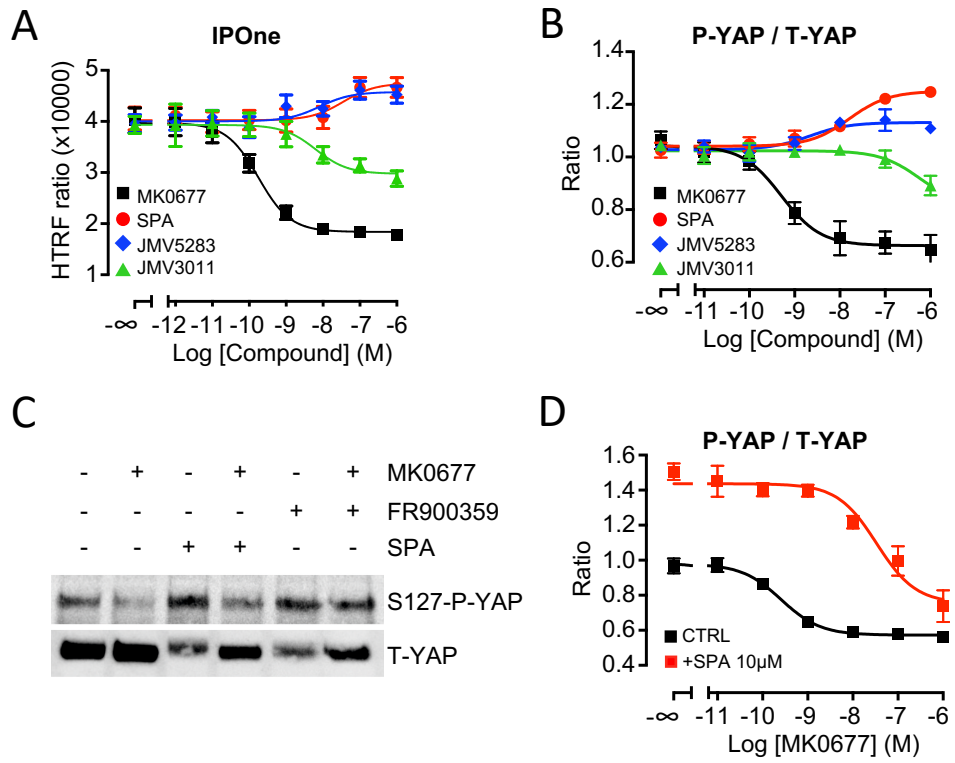


Figure 4

Figure 5

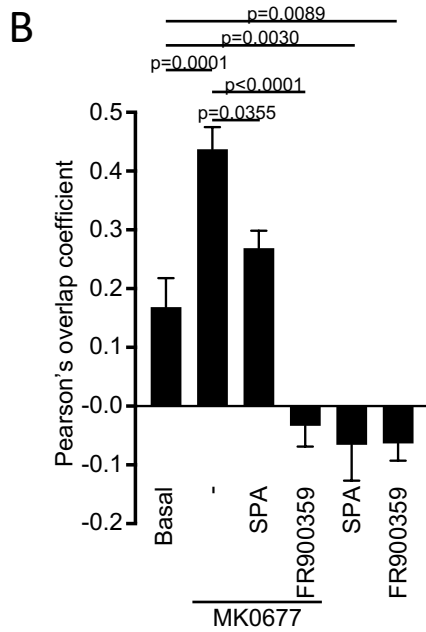
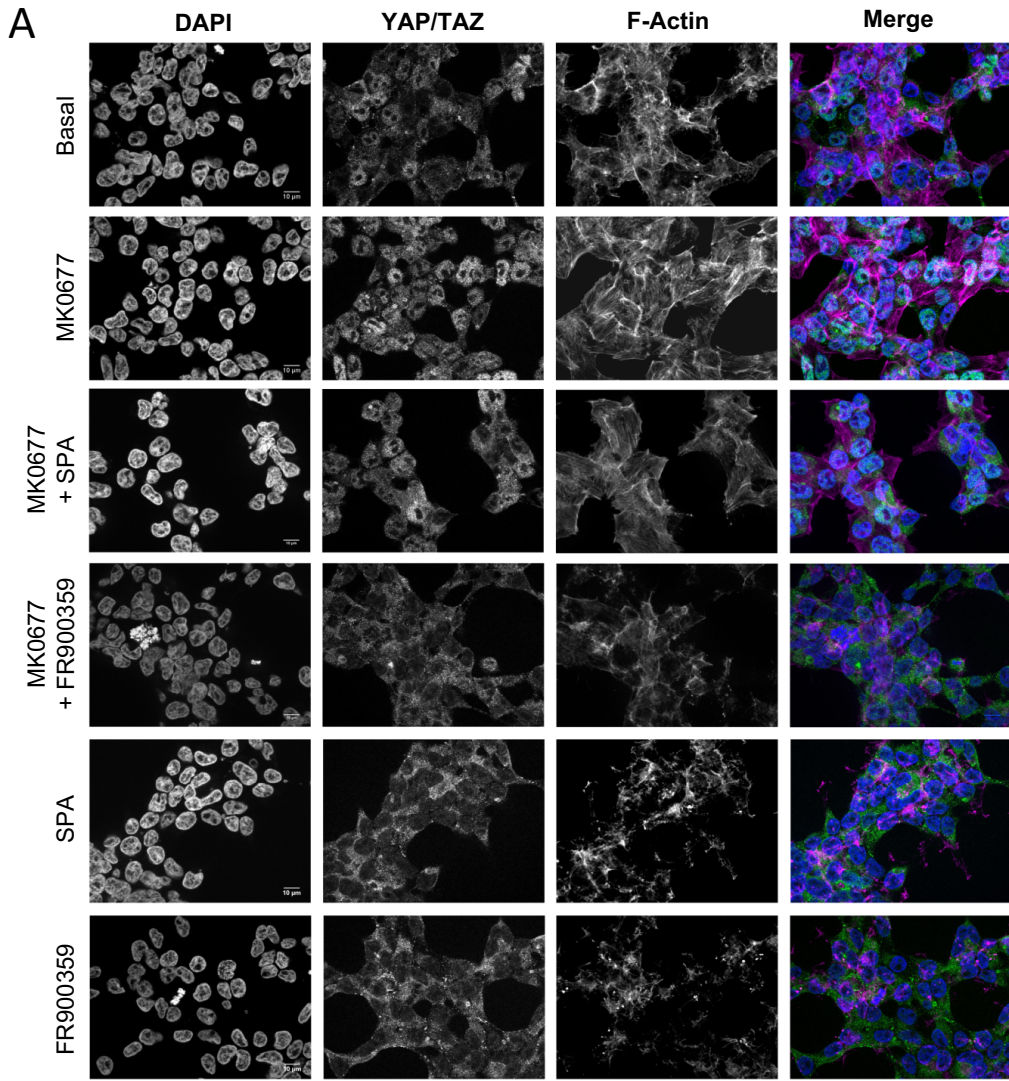


Figure 5

Figure 6

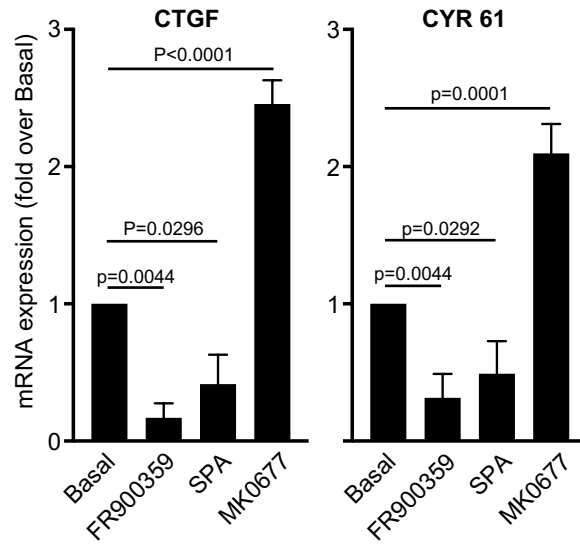


Figure 6

Figure 7

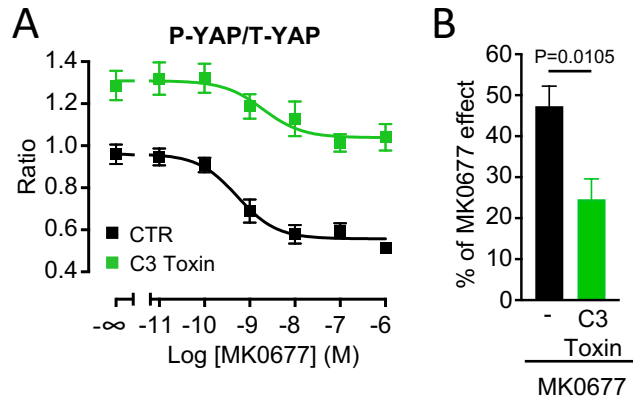


Figure 7

Figure 8

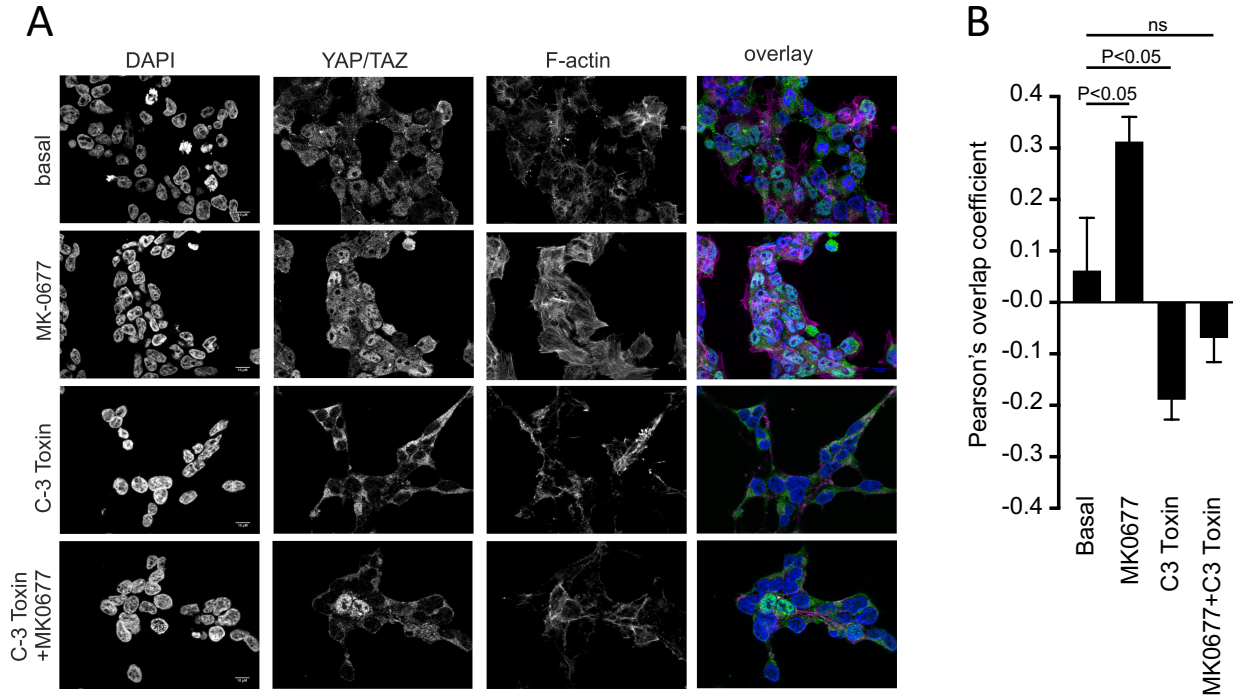


Figure 8

Supplementary Data

Legends of SuppFigures

SuppFig1: Assessment of S127 YAP dephosphorylation in HEK293 cells using innovative HTRF®-based assays. **A** Total and phosphorylated S127 YAP levels and the ratio P-YAP/T-YAP were assessed at different times using the Total-YAP (T-YAP) and Phospho-YAP (S127) (P-YAP) HTRF® kits, in overnight serum-starved HEK293 cells upon 10% serum stimulation. **B** YAP, TAZ and YAP-S127 proteins were detected at different times using western blot techniques, in overnight serum-starved HEK293 cells upon 10% serum stimulation. The anti YAP antibody is also recognizing the YAP-related TAZ protein. **C** As in **A**, phosphorylation of S127 YAP was detected at different times using P-YAP T-YAP HTRF® kits and analyzed using the ratio P-YAP/T-YAP, in HEK293 cells upon 10% serum or S1P (1 μ M) stimulation after OVN serum starvation. These data are representative of three independent experiments.

SuppFig.2: Ghrelin receptor GHS-R1a expressed in GHS-R1a HEK293 stable cell line. **A** After labeling the SNAP-domain inserted at the N-terminal end of the GHS-R1a receptor with Terbium cryptate HTRF® donor lumiphore, the binding experiments were performed in the GHS-R1a HEK293 cells by assessing the HTRF signal between the donor Terbium lumiphore and the Ghrelin 1A receptor HTRF® acceptor Red Agonist (Cisbio, Codolet, France). The specific binding data were obtained by subtraction of the non-specific binding data obtained by co-incubation with the competitive compound Ghrelin at 10 μ M, from the total binding data of the Ghrelin receptor Red Agonist for each concentration of the Ghrelin receptor Red Agonist. **B** Competitive displacement of the Ghrelin 1A receptor Red Agonist (3.1nM) by Ghrelin and MK0677 in GHS-R1a HEK293 cells. These data are representative of at least three independent experiments.

SuppFig3: GHS-R1a stimulation induces YAP S127 dephosphorylation through Gq. GHS-R1a HEK293 cells were transfected or not (nt) with siRNAs targeting G α 12/13 (siG α 12/13), or with control siRNAs (Ctr siRNA). The next day, cells were serum-starved overnight, then pretreated or not with 10 μ M SPA or 1 μ M FR900359, and subsequently stimulated with the indicated concentration of MK0677 for 30 min at 37°C. Cells were lysed and assessed for S127 YAP phosphorylation (P-YAP) (**Left panel**) and for total YAP protein relative amount (T-YAP) (**Right panel**). Results are the mean \pm SEM of three independent experiments.

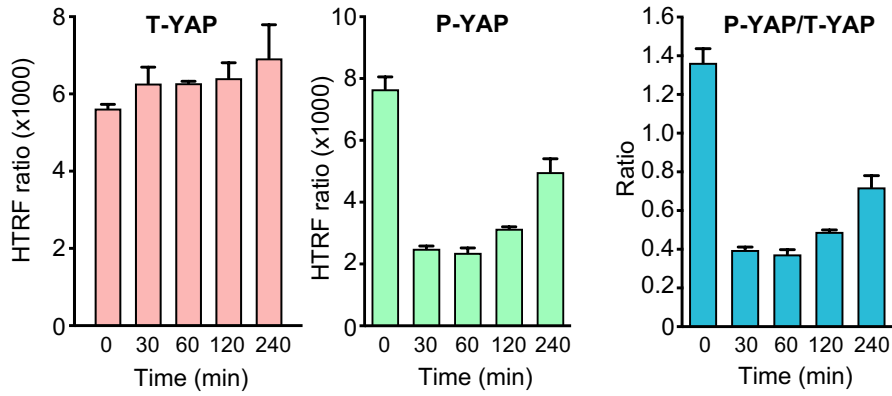
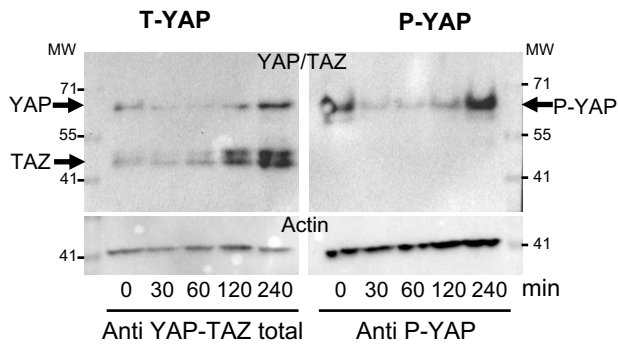
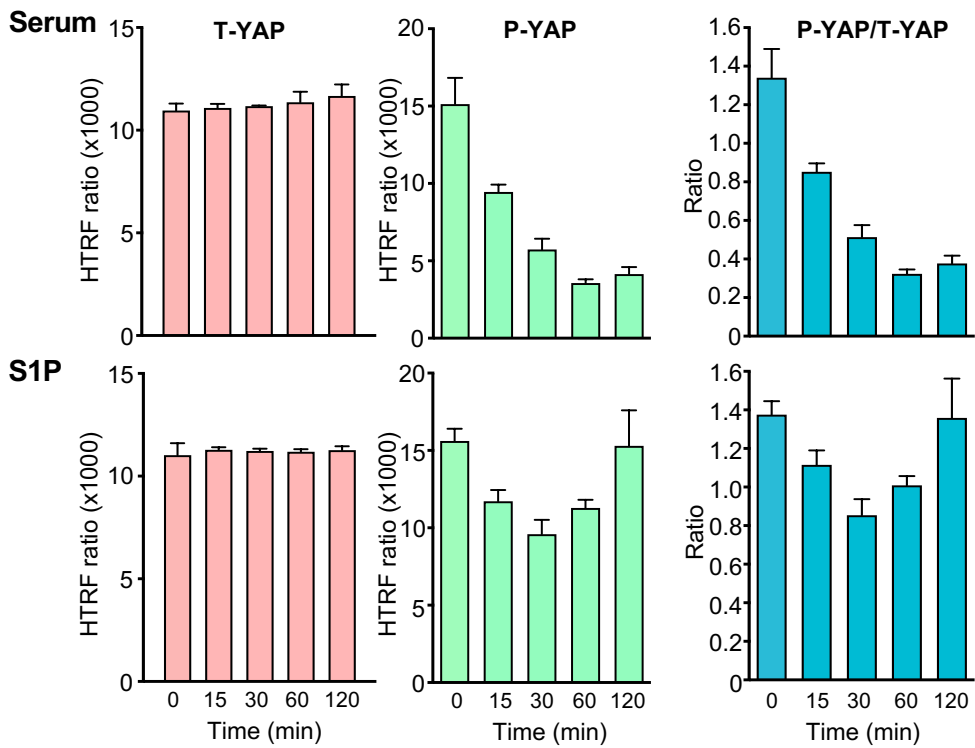
SuppFig4: GHS-R1a stimulation induces YAP S127 dephosphorylation independently of Gi/o pathway. **A** GHS-R1a HEK293 cells were transfected or not with the indicated siRNA against G α 12/13. Cells were serum-starved overnight then pretreated or not with PTX for 16 h (500 ng) or FR900359 for 1 hour (1 μ M) and subsequently stimulated with increasing concentrations of MK0677 for 30 min at 37°C. Cells were lysed and assessed for S127 YAP phosphorylation (P-YAP). **B** Cells were treated the same way as in **A**, but the effect of MK0677 was assessed for Erk1/2 protein phosphorylation using the Advanced ERK phospho-T202/Y204 kit (Cisbio). Results are representative of three independent experiments.

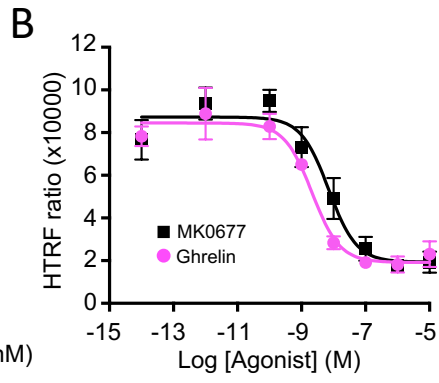
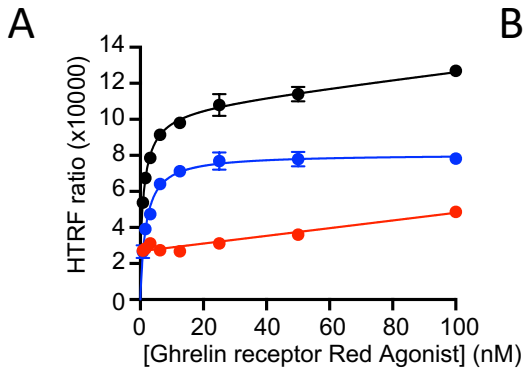
SuppFig5: S1P triggers S127 YAP dephosphorylation through both Gα12/13 and Gαq pathways in GHS-R1a HEK293 cells. GHS-R1a HEK293 cells transfected or not (nt) with siRNAs targeting Gα12/13 (siGα12/13), or with control siRNAs (Ctr siRNA) were starved overnight and pretreated or not with 1 μM FR900359 for 1 hour at 37°C and then stimulated with increasing concentrations of S1P for 30 min at 37°C. Subsequently cells were lysed and analyzed for S127 YAP phosphorylation (P-YAP) (**Left panel**) and total YAP relative protein amount (T-YAP) (**Right panel**). Results are the mean ± SEM of at least three experiments.

SuppFig6: GHS-R1a dual control of YAP S127 phosphorylation through both agonist-induced and agonist-independent activity. **A** Phosphorylated S127 YAP (**Left panel**) and total YAP relative protein amount (T-YAP) (**Right panel**) were assessed using HTRF® assays in GHS-R1a HEK293 cells after 30 min treatment with increasing concentrations of MK0677, SPA, JMV5289, or JMV-3011. Results are the mean ± SEM of three experiments. **B** Cells were activated by MK0677 in the absence or the presence of a 10 μM concentration of SPA, and then analyzed for S127 YAP phosphorylation (P-YAP) (**Left panel**) or total YAP relative protein amount (T-YAP) (**Right panel**). Results are the mean ± SEM of three experiments.

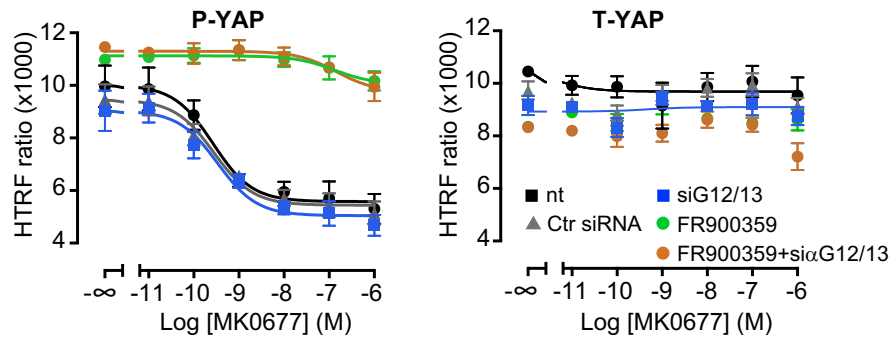
SuppFig.7: MK0677-induced YAP dephosphorylation involves Rho pathway

(A) GHS-R1A HEK293 cells were starved overnight and treated or not with 2 μg/ml botulinum toxin C3 for 16 h and subsequently analyzed for phosphorylated YAP (P-YAP) (**Left panel**) and total YAP relative protein amount (T-YAP) (**Right panel**) after MK0677 treatment using HTRF® assays.

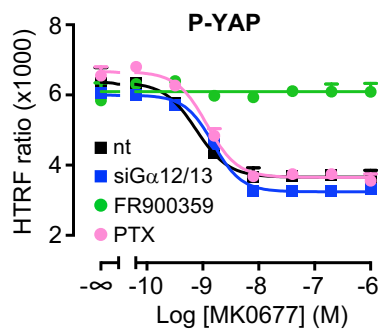
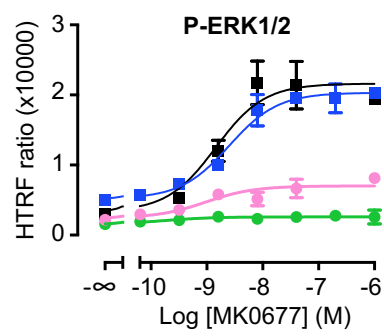
A**B****C**



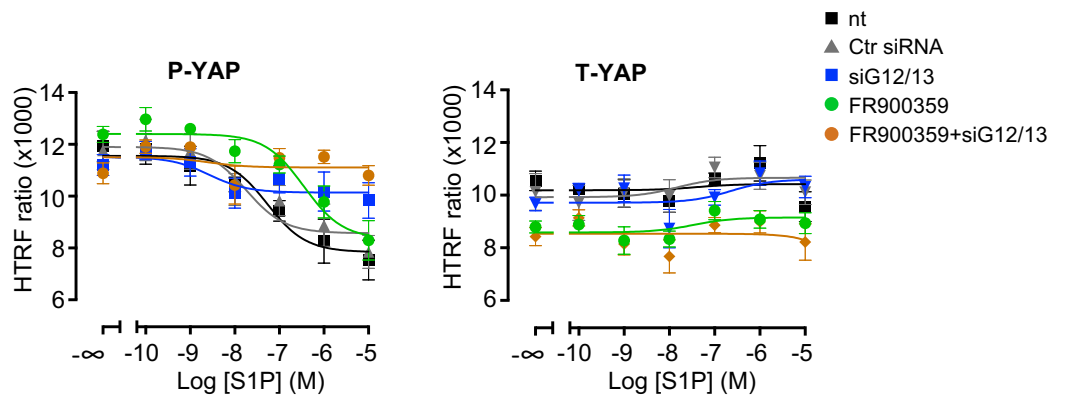
SuppFig.2



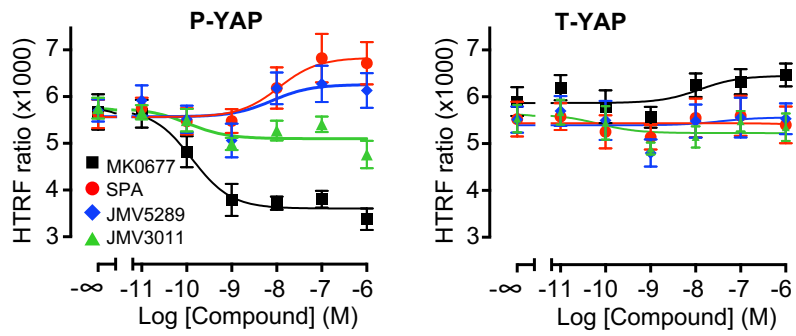
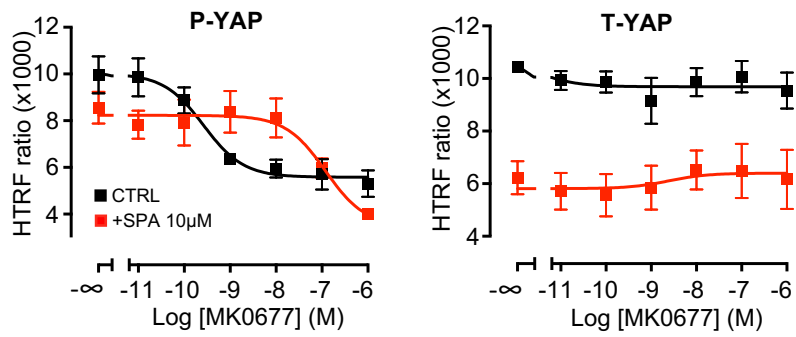
SuppFig.3

A**B**

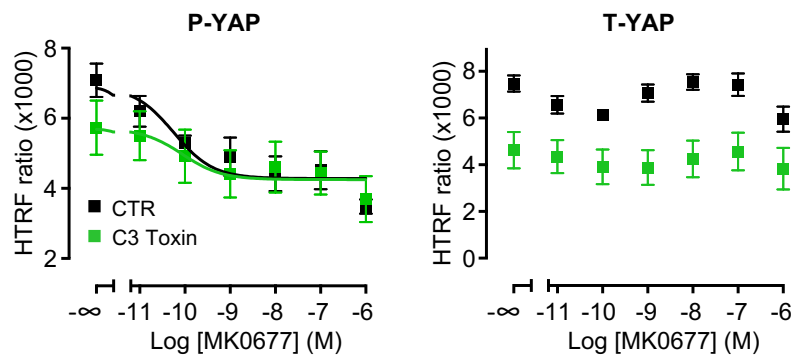
SuppFig.4



SuppFig.5

A**B**

SuppFig.6



SuppFig.7